Deep level transient spectroscopy and photoluminescence studies of hole and electron traps in $ZnSnP_2$ bulk crystals

Taro Kuwano,[1] Ryoji Katsube,[1] Steve Johnston,[2] Adele C. Tamboli,[2] Yoshitaro Nose[1]*

[1] *Department of Materials Science and Engineering, Kyoto University, Kyoto, Japan*

[2] *National Renewable Energy Laboratory, Golden, Colorado 80401, USA*

*E-mail: nose.yoshitaro.5e@kyoto-u.ac.jp

Abstract (less than 100 words)

$ZnSnP_2$, an emerging inorganic material for solar cells, was characterized by deep level transient spectroscopy (DLTS) and photoluminescence (PL). Acceptor- and donor-like traps with shallow energy levels were detected by DLTS analysis. The previous study based on first-principle calculation also suggested such traps were due to antisite defects of Zn and Sn. PL measurements also revealed sub-gap transitions related to these trap levels. Additionally, DLTS found a trap with deep level in $ZnSnP_2$. A short lifetime of minority carrier in previous work might be due to such trap, coming from phosphorus vacancies and/or zinc interstitials suggested by first-principle study.

$ZnSnP_2$ (ZTP) has recently attracted much attention as a photo-absorber of thin-film solar cells because of the non-toxic constituents, the suitable bandgap (1.67 eV), and the high absorption coefficient of about 10^5 cm^{-1} in the visible light region.[1,2] Nakatsuka et al. first demonstrated solar cells using ZTP bulk crystals with the device structure of Al-doped ZnO/CdS/ZTP/Mo referring to the typical structure of $CuInSe_2$-based solar cells, and reported the conversion efficiency of 0.087%.[3] They also discussed the high series resistance of 100 Ω cm^2 in the above device and proposed the usage of Cu as a back electrode in order to reduce the resistance in the subsequent work.[4] Based on their results, we recently revealed the formation of intermediate compound Cu_3P , which is well-matched to ZTP in the viewpoints of band and lattice structures, between ZTP and Cu electrode by heat treatment. Moreover, we have achieved 1.5 Ω cm^2, comparable to the resistance of the absorber ZTP, through the electrode structure with Cu_3P sputtered in advance, and consequently demonstrated the efficiency of 3.87% in ZTP solar cells.[5,6] On the other hand, there is still room for an efficiency improvement much, in particular, a short lifetime of minority carrier in ZTP bulk crystals reported by Nakatsuka et al.[3] The short circuit current density (J_{SC}) and open circuit voltage (V_{OC}) in the device with the best efficiency are 12.1 mA cm^{-2} and 0.535 V, respectively, and such low performance may come from poor carrier lifetime. The external quantum efficiency (EQE) spectra in ZTP also showed a strong bias dependence in longer wavelength region, and which indicated an insufficient carrier collection through light absorption in this wavelength region, in other words short diffusion length of minority carriers.

In this study, ZTP bulk crystals were characterized by deep level transient spectroscopy (DLTS) and photoluminescence (PL) for discussion on intrinsic defects to improve carrier lifetime. DLTS is well known to be a technique to detect trap levels in semiconductor, and also applied to devices recently. Das et al. demonstrated the existence of deep acceptor levels detected by DLTS in $Cu_2ZnSn(S_xSe_{1-x})_4$ (CZTSSe) solar cells directly affects the cell performance.[7] A further discussion including first-principle calculation on intrinsic point defects such as formation energies and energy levels is fruitful for conventional materials of thin-film solar cells[8] and even for emerging absorber materials such as SnS[9], Cu_3N[10], FeS_2[11], and Cu_2SnS_3[12]. Particularly, combination of experiments and theory based on defect physics is developing[13], and actually it was clearly shown that emission observed in PL spectrum consisted of some recombination processes related to shallow and deep levels in an absorber material $CuSbS_2$.[14] The aim of this study is thus to reveal the recombination behavior of minority carrier based on

energy levels due to intrinsic defects in ZTP through electric and optical evaluations, and theoretical calculation. Note that Kumagai et al. reported first-principle calculation for intrinsic point defects in ZTP and evaluated formation energy and energy level of each defect.[15] In this study, we discuss experimental results by DLTS, PL, and our previous results on time-resolved PL (TRPL) based on their calculation.

ZTP bulk crystals were grown by a solution method using Sn flux as reported by Nakatsuka et al.[16] The obtained bulk crystals were cut into wafers with the thickness of ~0.8 mm and both surfaces of each wafer were mechanically polished and chemically treated using 1/2-diluted aqua regia, 1/4-diluted hydrochloric acid, and ultrapure water in this order. For DLTS measurements, we prepared specimens with the structure of Ag/ZTP/Cu_3P/Cu, where Ag and Cu were adopted as a Schottky and ohmic contact, respectively.[4,5] Cu_3P thin layer with 25 nm in thickness was prepared on a treated surface by DC sputtering, and then Cu film was also deposited by DC sputtering in the same chamber. After deposition of Cu_3P and Cu, the specimens were annealed at 673 K for 5 min in evacuated quartz ampule to reduce the resistance. Subsequently, Ag electrode was prepared on the opposite surface of wafer by conventional thermal evaporation. According to a typical DLTS procedure proposed by Lang,[15] the transient capacitances between a certain time, t_1 and t_2, with various rate windows, expressed by ΔC, were evaluated as a function of temperature for Ag/ZTP/Cu_3P/Cu diodes. The reverse and pulse biases were set at −1.3 and 1.3 V for condition 1, and −1.7 and 1.7 V for condition 2, respectively. The pulse width was 1 ms for both conditions. The temperature was swept from 300 to 80 K. PL measurements were performed at room temperature using a He-Cd laser with the wavelength of 442 nm and the power of 10 mW.

Figure 1 shows DLTS signals for the Ag/ZTP/Cu_3P/Cu specimen measured under the conditions 1 and 2. A series of negative signals were observed in condition 1 as seen Fig. 1(a), while each spectrum in Fig. 1(b) for condition 2 includes negative and positive signals. Since ZTP exhibits a *p*-type conductivity,[9] Figure 1 indicates two acceptor-like (hole) traps, A1 and A2, and one donor-like (electron) trap, D1, in ZTP bulk crystal. According to conventional analysis for DLTS,[17,18] activation energy of trap *i*, E_i, is estimated using the following relation,

$$\tau T^2 \propto \exp\left(E_i / kT\right), \tag{1}$$

where T is the absolute temperature at which ΔC takes maximal or minimal value, k is the Boltzmann constant and τ is the time constant defined as

$$\tau = \frac{t_2 - t_1}{\ln(t_2 / t_1)} . \quad (2)$$

In this study, the ratio, t_2/t_1, was fixed at 11.5, hence τ equals to $4.3t_1$. Figure 2 shows an Arrhenius plot derived from DLTS. The activation energies for traps A1, A2, and D1 were estimated to be 0.12±0.01, 0.65±0.13, and 0.21±0.02 eV, respectively. The estimated energies for donor- and acceptor-like traps correspond to gaps with the conduction band minimum (CBM) edge, E_c, or the valence band maximum (VBM) edge, E_v. Diagram of relative energy levels for E_c, E_v, and traps is thus shown in Fig. 3. We first discuss the carrier recombination including shallow levels based on the diagram. Figure 4 shows PL spectrum of a ZTP wafer measured at room temperature. In Fig. 4, a sharp emission coming from band-to-band transition is observed around 1.69 eV, while emission with small and broad signal is confirmed in the lower energy range. Considering the diagram shown in Fig. 3, there are three transition processes in addition to band-to-band recombination in the energy range of PL measurements. We thus analyzed the PL spectrum using Voigt function assuming four transitions: D1 to A1 (DAP), D1 to VBM, CBM to A1, and band-to-band. The results are also shown as blue-dashed and green-solid lines in Fig. 4. Peak positions derived from four Voigt functions were 1.29, 1.41, 1.59, and 1.69 eV. The energies for four possible recombination processes in the diagram shown in Fig. 3 are 1.36 (E_{D1}–E_{A1}), 1.48 (E_{D1}–E_V), 1.57 (E_C–E_{A1}) and 1.69 eV (E_C–E_V), which correspond to the energies for respective transitions observed in PL spectrum. Therefore, the results of PL and DLTS coincide with each other. According to the calculation by Kumagai et al.[15], formation energies are significantly low for antisites of Zn on Sn site (Zn_{Sn}) and Sn on Zn site (Sn_{Zn}), suggesting that they are dominant defects in ZTP. Thermodynamic transition level, TTL, of Sn_{Zn} (+2/0) is 0.2 eV below CBM edge, which means antisite of Sn can act as a donor-like defect. On the other hand, antisite of Zn might act as acceptor and lead to *p*-type conductivity of ZTP although TTL of Zn_{Sn} (0/−2) was not clearly confirmed between CBM and VBM in the calculation. It is stated that the formation energy of Zn_{Sn}^0 was overestimated in their calculation resulting in lower TTL of Zn_{Sn}. The temperature dependence of hole concentration in ZTP is shown in Figure S1 for supplementary information, and the activation energy in *p*-type ZTP is evaluated to be 0.105 eV, which is supported the formation of Zn_{Sn} as an acceptor defect.

TTLs can be experimentally obtained from DLTS or temperature-dependent Hall effect measurements.[19] In DLTS, TTLs are evaluated from activation energies since corresponding to thermal

ionization energies.[20] Consequently, shallow traps of D1 and A1 come from antisite defects of Sn_{Zn} and Zn_{Sn}, respectively. We also discuss A2, the trap with deep level in the diagram shown in Fig. 3. In the viewpoint of TTL, similarly to the discussion for traps D1 and A1, vacancies of phosphorus and tin, and interstitial defects of zinc and phosphorus should be considered for A2. Among them, vacancy of phosphorus (V_P) and interstitial zinc (Zn_i) are rather favorable from their formation energies. First-principle calculation actually suggested that they might show acceptor-like behavior.

Here, we re-discuss a decay curve of TRPL in ZTP bulk crystal reported in our previous work.[3] They analyzed the curve using two components and evaluated minority carrier lifetime to be 0.442 and 37.8 ns. On the other hand, the ratio of the pre-exponential factors of fast component to slow one was about 10^2, which implies that almost all minority carriers with light-excited vanished due to fast recombination other than band-to-band. This experimental fact is consistent to the present results showing the presence of A2, the trap with deep energy level, based on the Shockley-Read-Hall theory.[21,22]

In summary, we investigated hole and electron traps in ZTP bulk crystals by DLTS and PL. DLTS analysis revealed three types of trap in ZTP bulk crystal: two with shallow energy levels and the other with deep level. Hole and electron traps with shallow levels are related to carrier concentration at room temperature, corresponding to so-called donor and acceptor defects, respectively. The previous study based on ab-initio calculation also suggested antisite Sn and Zn might correspond to such defects, respectively, which are favorable in the viewpoint of the formation energy. In the PL spectrum, the sub-gap luminescence in broad energy range was observed, and it was understood the spectrum contained four transition related to CBM, VBM and the above acceptor and donor levels. On the other hand, the trap with deep energy level might come from phosphorus vacancy or Zn interstitials, and the presence of such trap is also suggested in TRPL decay of our previous work. The formation energy of such defects by calculation is relatively high in ZTP and it is advantage as an absorber in solar cells. However, the discussion on DLTS is slightly inconsistent with theoretical studies. This might be from chemical environment, in other words chemical potentials of constituent elements, in preparation of bulk crystals, which should be considered and investigated in future works.

Acknowledgments

The authors thank to Talysa Klein and Patricia Dippo (NREL) for their experimental contributions.

This study was supported by JST CREST Grant No. JPMJCR17J2 and JSPS KAKENHI Grant No. JP20H00302. Collaboration by NREL scientists A.C.T. and S.J. was supported by the U.S. Department of Energy (DOE) under contract number DE-AC36-08GO28308 and funded by the DOE Office of Science, Basic Energy Sciences, Materials Science and Engineering Division.

References

1) J. L. Shay and J. H. Wernick, *Ternary chalcopyrite semiconductors, growth, electronic properties, and applications* (Pergamon Pr, Oxford, 1975).

2) T. Yokoyama, F. Oba, A. Seko, H. Hayashi, Y. Nose, and I. Tanaka, Appl. Phys. Express **6**, 061201 (2013).

3) S. Nakatsuka, N. Yuzawa, J. Chantana, T. Minemoto, and Y. Nose, Phys. Status Solidi A **214**, 1600650 (2017).

4) S. Nakatsuka, S. Akari, J. Chantana, T. Minemoto, and Y. Nose, ACS Appl. Mater. Interfaces **9**, 33827 (2017).

5) T. Kuwano, R. Katsube, and Y. Nose, in *2019 IEEE 46th Photovoltaic Specialists Conference (PVSC)* (2019) pp. 3007.

6) T. Kuwano, R. Katsube, K. Kazumi, and Y. Nose, Sol. Energy Mater. Sol. Cells **221**, 110891 (2021).

7) S. Das, S. K. Chaudhuri, R. N. Bhattacharya, and K. C. Mandal, Appl. Phys. Lett. **104**, 192106 (2014).

8) J. S. Park, S. Kim, Z. Xie, and A. Walsh, Nat. Rev. Mater. **3**, 194 (2018).

9) J. Vidal, S. Lany, M. d'Avezac, A. Zunger, A. Zakutayev, J. Francis, and J. Tate, Appl. Phys. Lett. **100**, 032104 (2012).

10) A. Zakutayev, C. M. Caskey, A. N. Fioretti, D. S. Ginley, J. Vidal, V. Stevanovic, E. Tea, and S. Lany, J. Phys. Chem. Lett. **5**, 1117 (2014).

11) L. Yu, S. Lany, R. Kykyneshi, V. Jieratum, R. Ravichandran, B. Pelatt, E. Altschul, H. A. S. Platt, J. F. Wager, D. A. Keszler, and A. Zunger, Adv. Energy Mater. **1**, 748 (2011).

12) P. W. Guan and Z. K. Liu, Phys. Chem. Chem. Phys. **20**, 256 (2018).

13) A. Alkauskas. M. D. McCluskey, and C. G. Van de Walle, J. Appl. Phys. **119**, 181101 (2016).

14) F. W. de Souza Lucas, H. Peng, S. Johnston, P. C. Dippo, S. Lany, L. H. Mascaro, and A. Zakutayev, J. Mater. Chem. A **5**, 21986 (2017).

15) Y. Kumagai, M. Choi, Y. Nose, and F. Oba, Phys. Rev. B **90**, 125202 (2014).

16) S. Nakatsuka, H. Nakamoto, Y. Nose, T. Uda, and Y. Shirai, physica status solidi c **12**, 520 (2015).

17) D. V. Lang, J. Appl. Phys. **45**, 3023 (1974).

18) D. K. Schroder, *Semiconductor Material and Device Characterization, 3rd ed.* (John Wiley & Sons, Inc., New Jersey, 2015), pp. 270–274.

19) C. Freysoldt, B. Grabowski, T. Hickel, J. Neugebauer, G. Kresse, A. Janotti, and C. G. Van de Walle, Rev. Mod. Phys. **86**, 253 (2014).

20) D. Wickramarantne, C. E. Dreyer, B. Monserrat, J.X. Shen, J. L. Lyons, A. Alkauskas, and C. G. Van de Walle, Appl. Phys. Lett. **113**, 192106 (2018).

21) W. Shockley and W. T. Read, Phys. Rev. **87**, 835 (1952).

22) R. N. Hall, Phys. Rev. **87**, 387 (1952).

Figure Captions

Fig. 1. DLTS spectra of Ag/ZTP/Cu_3P/Cu specimen with various t_1. Reverse bias and pulse bias are (a) −1.3 and 1.3 V and (b) −1.7 and 1.7 V, respectively.

Fig. 2. Arrhenius plots from DLTS spectra of Ag/ZTP/Cu_3P/Cu specimen shown in Fig. 1.

Fig. 3. Energy levels by DLTS analysis shown with respect to CBM and VBM.

Fig. 4. Room-temperature PL spectrum of a ZTP bulk crystal.

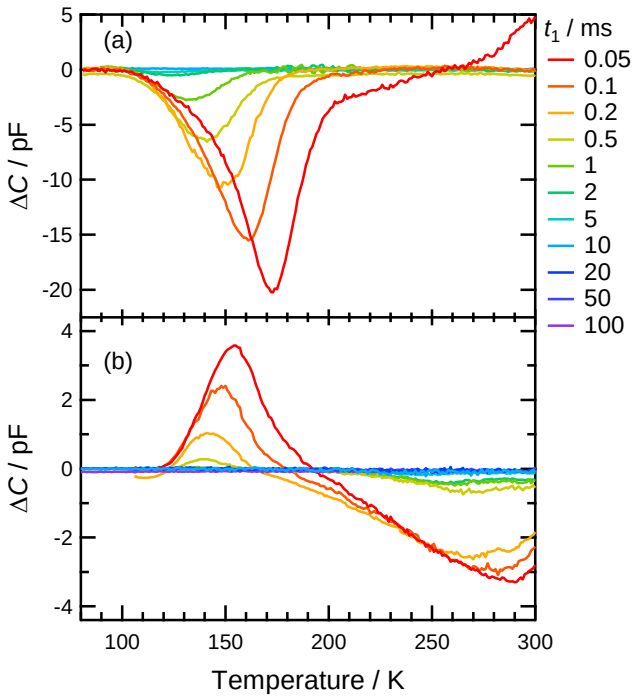

Fig. 1. DLTS spectra of Ag/ZTP/Cu_3P/Cu specimen with various t_1. Reverse bias and pulse bias are (a) −1.3 and 1.3 V and (b) −1.7 and 1.7 V, respectively.

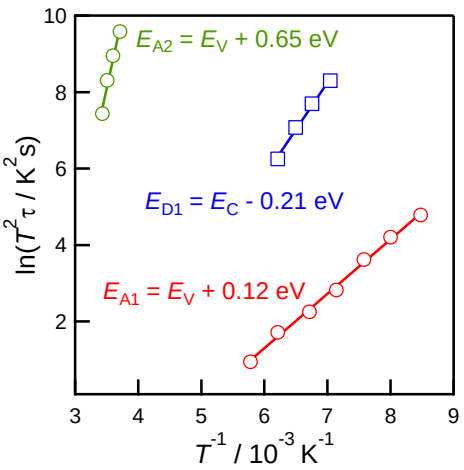

Fig. 2. Arrhenius plots from DLTS spectra of Ag/ZTP/Cu_3P/Cu specimen shown in Fig. 1.

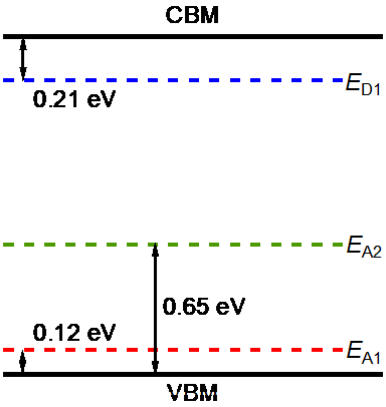

Fig. 3. Energy levels by DLTS analysis shown with respect to CBM and VBM.

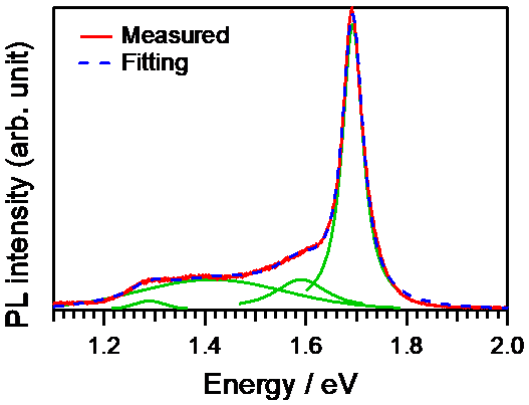

Fig. 4. Room-temperature PL spectrum of a ZTP bulk crystal.